Axisymmetric Boundary Layers

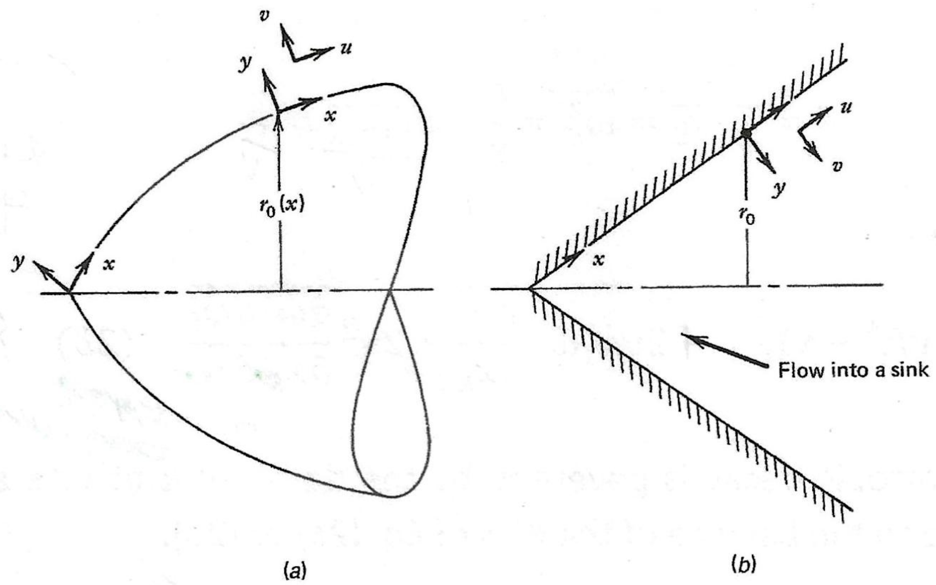

Figure 20.20 Nomenclature for Mangler's transformation: (*a*) axisymmetric boundary layer and (*b*) flow into a conical passage.

Assume no swirl and δ is small vs. both longitudinal and transverse radius of curvature. Boundary layer equations derived by Mangler (1945), which differ from 2D planar case by the appearance in the continuity equation of r_0:

$$\frac{\partial}{\partial x}(r_0 u) + r_0 \frac{\partial v}{\partial y} = 0$$

$$u\frac{\partial u}{\partial x} + v\frac{\partial u}{\partial y} = -\frac{1}{\rho}\frac{\partial p}{\partial x} + \nu\frac{\partial^2 u}{\partial y^2}$$

$$0 = \frac{\partial p}{\partial y}$$

$$-\frac{1}{\rho}\frac{\partial p}{\partial x} = u_e\frac{du_e}{dx}$$

Mangler also gave a mathematical transformation that transforms the axisymmetric problem into an equivalent plane problem.

$$x' = \int_0^x \left(\frac{r_0}{L}\right)^2 dx \qquad y' = \frac{r_0 y}{L}$$

$$u' = u \qquad U'(x') = U(x) \qquad v' = \frac{L}{r_0}\left(v + \frac{yu}{r_0}\frac{dr_0}{dx}\right)$$

Where L is an arbitrary length scale. Substitution into axisymmetric boundary layer equations [$\frac{\partial x'}{\partial \mathrm{x}} = \left(\frac{r_0}{L}\right)^2$ and $\frac{\partial y'}{\partial \mathrm{x}} = \frac{y}{L}\frac{\partial r_0}{\partial \mathrm{x}}$] produces the plane flow boundary layer equations:

$$\frac{\partial u'}{\partial x'} + \frac{\partial v'}{\partial y'} = 0$$

$$u'\frac{\partial u'}{\partial x'} + v'\frac{\partial u'}{\partial y'} = U'\frac{\partial U'}{\partial x'} + \nu\frac{\partial^2 u'}{\partial y'^2}$$

A solution of an axisymmetric boundary layer may be found by considering an equivalent plane boundary layer vis Mangler's transformation. When r_0 is constant the transformation is trivial.

As an example, consider axisymmetric stagnation point on a blunt body: Homann flow. The inviscid velocity near the stagnation point is given by,

$$\frac{u_e}{u_0} = \frac{x}{L} \qquad u_0 = \alpha u_\infty$$

L = characteristic body dimension and α depends on the shape of the body. For $r_0 = x$,

$$\frac{x'}{L} = \int_0^{x/L} \left(\frac{r_0}{L}\right)^2 d\,\frac{x}{L} = \frac{1}{3}\left(\frac{x}{L}\right)^3$$

$$\frac{y'}{L} = \frac{r_0}{L}\frac{y}{L} = \frac{x}{L}\frac{y}{L}$$

Which define the point x', y' in the plane flow, which is equivalent to the point x, y in the axisymmetric flow. Next transform the external velocity,

$$u_e' = u_e$$

$$\frac{u_e'}{u_0} = \frac{x}{L} = \left(3\frac{x'}{L}\right)^{1/3}$$

The equivalent plane flow is, $u_e \approx x'^{1/3}$ where the reference velocity constant is unchanged, but the length constant is $\frac{L}{3} = L'$.

The solution to a boundary layer obeying the $\frac{x'}{L}$ and $\frac{y'}{L}$ is the Falkner-Skan flow for m=1/3 ($\theta_{1/2} = 45^\circ$ wedge). Assuming that this solution is known, the u velocity at the point x, y in the axisymmetric stagnation point flow would be,

$$\frac{u(x,y)}{u_0} = f'\left[\frac{y'}{L} \to \frac{x}{L}\frac{y}{L}, \frac{x'}{L} \to \left(\frac{1}{3}\frac{x'}{L}\right)^3\right]$$

A corresponding formula for v is found from $v' = \frac{L}{r_0}\left(v + \frac{yu}{r_0}\frac{dr_0}{dx}\right)$. An axisymmetric stagnation point is 80% as thick as a plane stagnation point.

The flow toward a axisymmetric stagnation point is a special case of the streaming flow over a cone of a given angle. Since the external flow over a code obeys $u_e \propto x^n$ and the surface position is $r_0 = x sin\theta_{1/2}$, Mangler's transformation produces $u' \propto x^{n/3}$, which is one of the Falkner-Skan solutions. Unfortunately, there is no simple relation between the code angle θ and the exponent n. Whitehead and Canetti (1950) prove a graphical relationship.

Three-dimensional boundary layers: flow driven by both p_x and p_z

$$u_x + v_y + w_z = 0$$

$$uu_x + vu_y + wu_z = -\frac{p_x}{\rho} + \nu u_{yy}$$

$$uw_x + vw_y + ww_z = -\frac{p_z}{\rho} + \nu w_{yy}$$

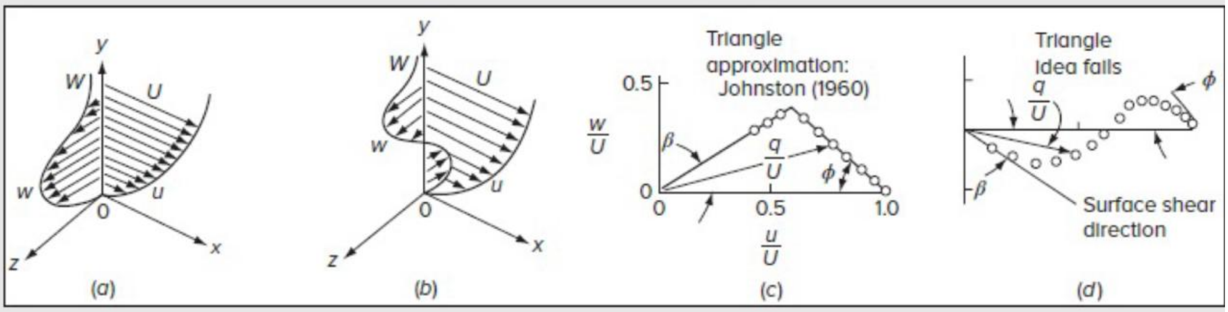

FIGURE 4-45

Unidirectional and bidirectional skewing in three-dimensional pressure-driven boundary layers: (*a*) unidirectional skewing; (*b*) bidirectional skewing; (*c*) unidirectional hodograph; (*d*) bidirectional hodograph.

Complex crossflow such as (b): death of 3D integral methods motivated 3D differential BL methods:

Three-dimensional turbulent boundary layers

- J. Nash, V. C. Patel
- Published 1972
- Physics, Engineering

Thick BL and separation led to rapid extensions differential methods to modern CFD: RANS, HRLES, LES, DNS.

Boundary layer with constant transverse pressure gradient: flat plate BL with parabolic free stream.

Flat plate with LE at $x = 0$ and inflow at angle θ_0

For $x > 0$ the BC at $y \to \infty$

$u \to u_e =$ constant $\qquad p_x = 0$

$w \to w_e = u_e(a + bx) \qquad -\frac{p_z}{\rho} = u_e w_{e,x} = u_e^2 b \qquad$ Euler equation

$b =$ magnitude transverse p_z

External flow $\underline{\omega} = \omega_y \hat{j} \qquad \omega_y = -\frac{\partial w}{\partial x} = -u_e b$

For $b = 0,\ \theta = \theta_0 = \tan^{-1}\left(\frac{w_e}{u_e}\right) = \tan^{-1} a$, which shows the effect of sweep on Blasius BL

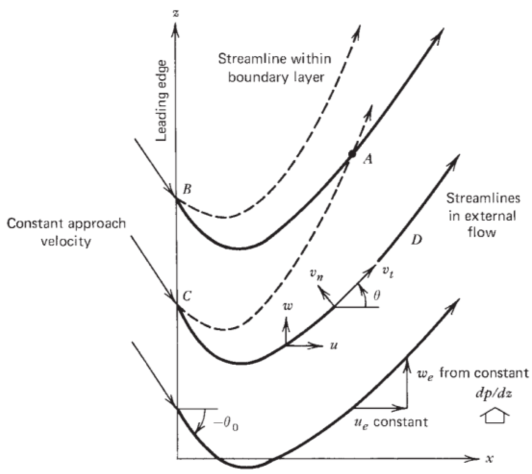

Figure 20.30 Plan view of the boundary layer on a plate with a constant transverse pressure gradient.

$\frac{dz_e}{dx} = \frac{w_e}{u_e} = a + bx \qquad z_e = ax + \frac{1}{2}bx^2 + c$

$c =$ constant $= z_e|_{LE}$

Concept of region of influence: particles that pass through c influence region *CAD*. 3D BL method must account for spreading lateral influence.

BL equations:

$u_x + v_y = 0$

$uu_x + vu_y = \nu u_{yy}$

$uw_x + vw_y = bu_0^2 + \nu w_{yy}$

continuity and x-momentum $\neq f(w)$ = Blasius BL problem

$\frac{u}{u_e} = f'(\eta) \qquad \eta = y\sqrt{\frac{u_e}{\nu x}}$

$f(\eta)$ solution Blasius equation: $ff'' + 2f''' = 0$

Sweep independence principle: u, v solved independent w

Assume: $\frac{w}{u_e} = \underbrace{\frac{w_e(x)}{u_e} f'(\eta)} + bx\, h(\eta)$

Blasius component scaled to match $w_e(x)$

Substitution in w-momentum equation

$\left.\begin{array}{c} h'' + \frac{1}{2} f h' - f'h + 1 - f'^2 = 0 \\ h(0) = h(\infty) = 0 \end{array}\right\}$ Similarly, Blasius equation solved numerically

Solutions use normal and tangential coordinates to outer flow and normalized with outer flow velocity magnitude $V_\infty = [u_e^2 + w_e^2]^{1/2}$

$$\frac{v_t}{V_\infty} = f'(\eta) + \frac{1}{2}\sin 2\,\theta\,(\tan\theta - \tan\theta_0)\,h(\eta)$$

$$\frac{v_n}{V_\infty} = \frac{1}{2}\cos^2\theta\,\,(\tan\theta - \tan\theta_0)\,h(\eta)$$

θ= local inviscid ψ angle $\tan^{-1}(w_e/u_e)$

(1) flat plate with sweep angle $\theta = \theta_0$ and $b = 0$

Blasius profile and no secondary flow, i.e., $v_n = 0$

If ψ_e coincides with the surface geodesic curves $\psi_{BL} = \psi_e$ and no secondary flow

Geodesic curve: curve whose tangent vectors remain parallel if they are transported along it

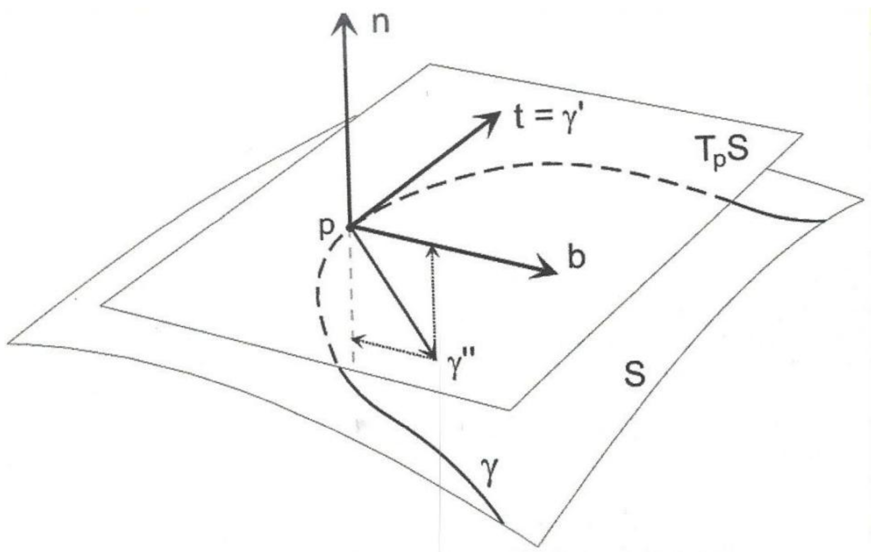

(2) $\theta \neq \theta_0$ and $b \neq 0$

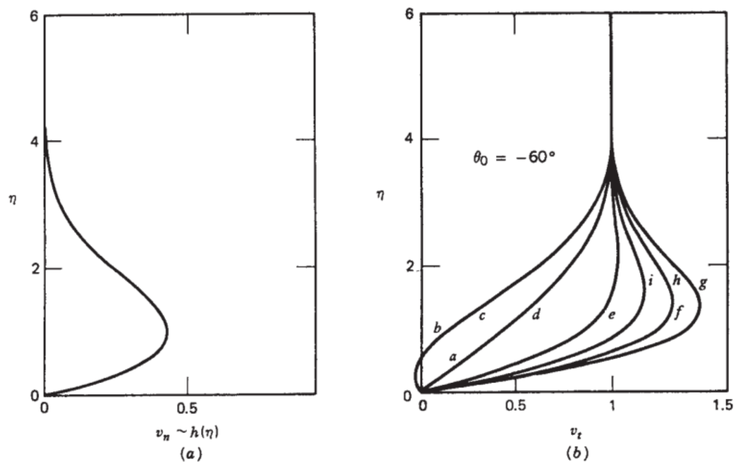

Figure 20.31 Typical velocity profiles: (*a*) transverse profiles $h(\eta)$; and (*b*) tangential profiles for various flow angles: $a, \theta = -60°$; $b, \theta = -40°$; $c, \theta = -20°$ (same curve as *b*); $d, \theta = 0°$ (same as *a*); $e, \theta = 20°$; $f, \theta = 40°$; $g, \theta = 60°$; $h, \theta = 80°$ (same as *f*); $i, \theta = 90°$.

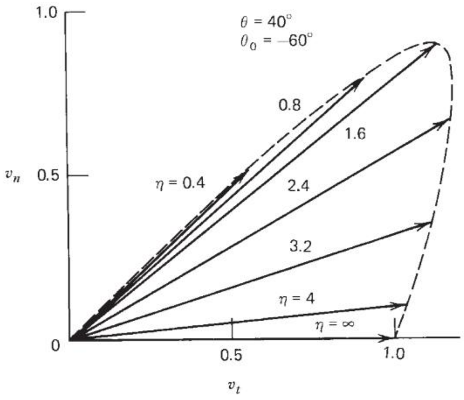

Figure 20.32 Polar diagram of velocity profile with overshoot.

v_n not shown since $\propto h(\eta)$

θ		
-60	a	Blasius
-40	b	
-20	c	
0 =a	d	Blasius
20	e	
40	f	
60	g	
$80 = f$	h	
90	I	

(for b, c) ⇒ $v_t < 0$ near $\eta = 0$, but not reverse flow
v_n large such that flow > 0 in x direction

(for g) ⇒ v_t exhibits overshoot in upper BL occurs frequently in 3D BL in this region (similar as Stokes 2nd problem for oscillating outer flow) net transverse viscous force some direction pressure force. Viscous force dies out at large η

Note: flow never actually separates

Surface streamlines:

$$z_s = ax + \frac{1}{2}bx^2\left[1 + \frac{h'(0)}{f''(0)}\right] + C_0$$ also, parabolas and differs z_e by

$$1 + \frac{h'(0)}{f''(0)} \approx 1 + \frac{1}{3}$$